could be a drawback of the present system when it is used for technological applications. Photoinduced phase transition, however, may be triggered not only by the ionization process as presented in this paper but by molecular conformational changes such as cis–trans isomerization. In that case it will be possible to control both the swelling and shrinking by using two lights with different wavelengths. We are currently studying various systems on the basis of this idea.

We believe that the work presented here is of technological importance in developing various optical devices, such as optical switches, display units, and three-dimensional holograms. The phase transition induced by light will also provide a means to carry out high-speed kinetic experiments of volume changes in gels, where the perturbation time is extremely fast. According to the principle of kinetics of gels, the time needed for swelling and shrinking of a gel is proportional to the square of the characteristic linear dimension of a gel. It is expected that a spherical gel with a diameter on the order of micrometers will respond to environmental changes within milliseconds. In order to carry out such a fast kinetic experiment it is important that the environment be altered extremely rapidly. For this reason the light-induced phase transition will be important since the perturbation time is extremely fast.

Acknowledgment. We thank Professor Satoru Masamune for assistance in the ultraviolet irradiation experiment. This work has been supported by Kao Corporation.

References and Notes

(1) Tanaka, T. *Phys. Rev. Lett.* **1978**, *40*, 820.
(2) Tanaka, T.; Fillmore, D. J.; Sun, S.-T.; Nishio, I.; Swislow, G.; Shah, S. *Phys. Rev. Lett.* **1980**, *45*, 1636.
(3) Ilavsky, M. *Macromolecules* **1982**, *15*, 782.
(4) Hrouz, J.; Ilavsky, M.; Ulbrich, K.; Kopecek, J. *Eur. Polym. J.* **1981**, *17*, 361.
(5) Hirokawa, Y.; Tanaka, T. *J. Chem. Phys.* **1984**, *81*, 6379.
(6) Ohmine, I.; Tanaka, T. *J. Chem. Phys.* **1982**, *11*, 5725.
(7) Amiya, T.; Tanaka, T. *Macromolecules* **1987**, *20*, 1162.
(8) Tanaka, T.; Nishio, I.; Sun, S.-T.; Ueno-Nishio, S. *Science* **1982**, *218*, 467.
(9) Ilavsky, M.; Hrouz, J.; Ulbrich, K. *Polym. Bull.* **1982**, *7*, 107.
(10) Flory, P. J. *Principle of Polymer Chemistry*; Cornell University Press: Ithaca, NY, 1953.
(11) Irie, M.; Kungwatchakun, D. *Macromolecules* **1986**, *19*, 2476. *Makromol. Chem., Rapid Commun.* **1984**, *5*, 829.
(12) Hirotsu, S.; Hirokawa, Y.; Tanaka, T. *J. Chem. Phys.* **1987**, *87*, 1392.

Influence of Blend Compressibility on Extrapolated Zero-Angle Coherent Scattering and Spinodal: Limitations of RPA Analysis

Jacek Dudowicz[†] and Karl F. Freed*

The James Franck Institute and the Department of Chemistry, University of Chicago, Chicago, Illinois 60637. *Received June 12, 1989; Revised Manuscript Received July 31, 1989*

ABSTRACT: Three different statistical thermodynamic models of compressible binary polymer blends are used to compute the extrapolated zero-angle coherent scattering $S_{11}(0)$ by one of its components. The models are taken from Flory–Huggins theory, equation of state theories, and Dickman–Hall continuum modifications of lattice theories. The computed zero-angle scattering is analyzed using the conventional incompressible RPA model to produce the effective Flory interaction parameter, χ_{eff}. When input polymer–polymer interactions that are composition and molecular weight independent are used, the computed χ_{eff} values exhibit strong composition and molecular weight dependences, solely as a result of the inappropriateness of the incompressible blend model used to define χ_{eff}. The vanishing of the reciprocal of $S_{11}(0)$ is shown to describe the spinodal line for a compressible binary blend at constant volume, but this is found to differ from the constant-pressure spinodal line. While our computed χ_{eff} values display some composition-dependent trends observed experimentally, several others cannot be generated. Hence, future studies will investigate the influence of composition and molecular dependences of the polymer–polymer interactions on χ_{eff}. Nevertheless, the simplest models employed here focus on the need for analyzing experimental data with thermodynamically more faithful models than the incompressible RPA if the desire is to obtain fundamental molecular information concerning basic polymer–polymer interactions in a blend.

I. Introduction

Theories of the structure and thermodynamics of polymer blends have been of considerable interest in ascertaining those characteristics promoting mixing or producing particular morphologies of phase-separated systems. These theories have been used in conjunction with neutron-scattering data and Monte Carlo simulations to provide an important tool in studies of the effective interaction parameter that governs the phase behavior of polymer blends. Extrapolated zero-angle neutron-scattering data provides a direct approach to the blend polymer–polymer interaction parameter, but the extraction of this effective interaction parameter is based on the use of random-phase approximation (RPA)[1] that assumes blend incompressibility. While the zero scattering angle limit of the RPA agrees with incompressible Flory–Huggins theory,[2] there are several reasons why the incompressible RPA model obscures essential physics of blends, such that the extracted effective interaction parameter does

[†] On leave from the Institute of Physical Chemistry of the Polish Academy of Sciences, 01-224 Warsaw, Poland.

0024-9297/90/2223-1519$02.50/0

not have the desired molecular interpretation.

Blends are liquids and therefore must be compressible. Polymer melt compressibilities are comparable to those of the monomeric liquids.[3] Hence, the melts and blends contain free volume that contributes to the entropy of the system and that can, in principle, affect the thermodynamic properties obtained from the extrapolated zero-angle coherent scattering experiments. This free-volume entropy is related to some of the so-called "equation of state terms" in the equation of state theories,[4] and clearly similar contributions must arise in polymer blends.

Recently, there have been a few treatments[5-7] that include the free volume and that are shown here to describe "semi-compressible" polymer blends in which the free volume is taken to be independent of blend composition because the treatments neglect interaction parameters that account for the large free energy cost of producing free volume. Freed[5] and Sariban and Binder[6] apply Flory–Huggins theory of such a semi-compressible binary blend to evaluate the extrapolated zero-angle neutron-scattering structure factor $S(\mathbf{q}=0)$ and the associated Flory effective interaction parameter χ_{eff}. Freed[5] shows how both the composition and molecular weight dependence of χ_{eff} can be greatly altered from the standard incompressible RPA analysis when due cognizance is taken of the presence of free volume. An Edwards style compressible RPA treatment by McMullen and Freed[7] produces the same $\mathbf{q} \to 0$ limit as in refs 5 and 6 and thereby supports these previous thermodynamic models.

This paper studies the effective interaction parameter, χ_{eff}, for a fully compressible blend in which there is free volume and in which its variation has an associated change in free energy. Thus, the amount of free volume is composition dependent and may be eliminated from the theory, for instance, by use of the equation of state. Three different models are employed to describe the free-volume contribution to the free energy, namely, Flory–Huggins theory,[2] theories in the spirit of Flory's equation of state theory,[4] and the Dickman–Hall molecular liquid theory formulation[8] for correcting deficiencies of lattice models. Because of the presence of free volume in, for instance, the Flory–Huggins lattice model, there are now three independent interaction energies ϵ_{11}, ϵ_{22}, and ϵ_{12}. Our analysis departs from the prior one-interaction parameter RPA treatment of χ_{eff} by including all three interactions and their effect on the customary incompressible RPA analysis.

Section II outlines the theoretical background, discusses three models studied, and derives a new expression for the customarily defined χ_{eff}. Section III provides graphs depicting how the traditionally defined χ_{eff} depends on blend composition, molecular weights, the ϵ_{ij}, free volume, and the model employed, even when the original interaction energies ϵ_{ij} are independent of composition, molecular weight, and free volume. Section IV contrasts the phase stability conditions for a single homogeneous phase in compressible blends at constant volume and at constant pressure and describes the spinodal diagrams for these two cases. Our results have a bearing on the use of experimental χ_{eff} to predict the location of spinodals.

II. Effective Flory Parameter, χ_{eff}, for Extrapolated Zero Angle Neutron Scattering from Compressible Blends

Neutron-scattering experiments[9] are a powerful tool for studying the nature of molecular interactions in polymer blends. The extrapolated zero scattering angle structure factor yields the effective monomer–monomer interaction parameter χ_{eff} that provides one measure of the molecular interactions in the blend and that appears also in theories of polymer interfaces and phase-separation dynamics. On the other hand, this χ_{eff} is also a purely thermodynamic parameter that may be evaluated from statistical thermodynamics.

We study the influence of blend compressibility on χ_{eff} by considering three models of the blend thermodynamic properties that are designed to exhibit the robust nature of our conclusions. The first model is the Flory–Huggins mean-field approximation[2] to the lattice model in which lattice sites are either occupied by one monomer of the self-avoiding polymers or are empty. These empty sites, called voids, represent free volume, whose presence characterizes the liquid state and makes the liquid compressible. Other models for the free-volume contribution to the blend entropy of mixing are considered based on the equation of state theories[4] and on the Dickman–Hall approaches[8] for rectifying deficiencies of lattice models by use of theories and simulations for small-molecule fluids. Theories that include corrections[10] beyond the Flory–Huggins (FH) approximation are left for future study of the influence of monomer structure on χ_{eff}.

Since neutron-scattering experiments are performed with a constant scattering volume, we consider the Helmholtz free energy, F. All of the three models studied have the compressible binary blend free energy given by

$$\frac{F}{N_1kT} = f_F(\phi_\nu) + \frac{\phi_1}{M_1}\ln\phi_1 + \frac{\phi_2}{M_2}\ln\phi_2 + g_{12}\phi_1\phi_2 + g_{1\nu}\phi_1\phi_\nu + g_{2\nu}\phi_2\phi_\nu + f_1\phi_1 + f_2\phi_2 \quad (2.1)$$

where N_1 is the total number of lattice sites, ϕ_i is the volume fraction of species i ($i = 1, 2$), M_i is the number of lattice sites occupied by chain of type i, and f_i is the specific free energy of pure species i per lattice site. The interaction parameters g_{ij} are related to the nearest-neighbor van der Waals attractive energies ϵ_{ij} as

$$g_{ij} = z(\epsilon_{ii} + \epsilon_{jj} - 2\epsilon_{ij})/2kT \quad (2.2)$$

where the void "interactions" obey $\epsilon_{\nu\nu} = \epsilon_{1\nu} = \epsilon_{2\nu} = 0$ because voids do not interact and where z is the lattice coordination number. The g_{ij} values are taken to be independent of composition, but future work will study the influence of their composition and molecular structure dependence. The function $f_F(\phi_\nu)$ is the contribution to the free energy F from the presence of free volume, and it is this function that differs between models treated.

FH theory expresses the free-volume contribution as

$$f_F^{FH}(\phi_\nu) = \phi_\nu \ln \phi_\nu \quad (2.3)$$

Equation of state theories,[4] on the other hand, attempt to describe the free-volume entropic contribution in a more realistic and elaborate way than the expression 2.3. These approaches distinguish between the total volume, V, and the close-packed volume, V^*. Here, we consider the simplest original Flory equation of state (FES) in which the free-volume contribution is

$$f_F^{FES}(\phi_\nu) = -3c(1-\phi_\nu)\ln[(1-\phi_\nu)^{-1/3} - 1] \quad (2.4)$$

where c is a phenomenological parameter and $\phi_\nu = (V - V^*)/V$.

Dickman and Hall[8] compare Flory–Huggins theory with the Carnahan–Starling equation of state of hard-sphere fluids[11] to develop what they call a generalized Flory equation of state. Their analysis is provided only for a single-component polymer system. A reasonable guessti-

mate of the extension of their simplest approach to a binary blend leads us to take

$$f_F^{DH}(\phi_\nu) = \left[a\left(\frac{1}{M_1}+\frac{1}{M_2}\right)+b\right]\left[\frac{1}{[1-\pi(1-\phi_\nu)/6]^2}+\ln\,[1-\pi(1-\phi_\nu)/6]^2\right] \quad (2.5)$$

where a and b are constants that depend on the excluded volume of polymer chain segments as modeled by hard spheres. Dickman and Hall[8] and Honnell and Hall[12] develop further equations of state that are more accurate and algebraically more complicated. These generalizations may be treated straightforwardly but more tediously by the analysis given below.

The chemical potentials μ_i, $i = 1, 2$, of each of two blend components are easily obtained by differentiating the free energy F with respect to number of chains n_i, giving

$$\frac{\mu_1}{M_1kT} = \left.\frac{\partial(F/M_1kT)}{\partial n_1}\right|_{V,T,n_2} = f_\mu(\phi_\nu) + \frac{\ln\phi_1}{M_1} + g_{12}\phi_2 + g_{1\nu}(\phi_\nu-\phi_1) - g_{2\nu}\phi_2 + \text{constant} \quad (2.6)$$

and

$$\frac{\mu_2}{M_2kT} = \left.\frac{\partial(F/M_2kT)}{\partial n_2}\right|_{V,T,n_1} = f_\mu(\phi_\nu) + \frac{\ln\phi_2}{M_2} + g_{12}\phi_1 - g_{1\nu}\phi_1 + g_{2\nu}(\phi_\nu-\phi_2) + \text{constant} \quad (2.7)$$

where

$$f_\mu^{FH}(\phi_\nu) = -\ln\phi_\nu \quad (2.8a)$$

$$f_\mu^{FES}(\phi_\nu) = -3c\,\ln\,[(1-\phi_\nu)^{-1/3}-1] + \frac{c}{1-(1-\phi_\nu)^{1/3}} \quad (2.8b)$$

$$f_\mu^{DH}(\phi_\nu) = \left[a'\left(\frac{1}{M_1}+\frac{1}{M_2}\right)+b'\right]\left[\frac{1}{[1-\pi(1-\phi_\nu)/6]^3}-\frac{1}{1-\pi(1-\phi_\nu)/6}\right] \quad (2.8c)$$

and a' and b' are constants.

The partial structure factor of one of two polymer species, say $S_{11}(0)$ (for scattering by monomers), is related to the chemical potential μ_1 by

$$S_{11}(0)^{-1} = \frac{N_1}{M_1kT}\left.\frac{\partial(\mu_1/M_1)}{\partial n_1}\right|_{V,T,\mu_2} \quad (2.9)$$

The derivative $\partial(\mu_1/M_1)/\partial n_1$ at constant chemical potential μ_2 may be expressed in terms of derivatives at a constant number of chains n_i through the thermodynamic identity

$$\left.\frac{\partial\mu_1}{\partial n_1}\right|_{V,T,\mu_2} = \left[\left.\frac{\partial\mu_1}{\partial n_1}\right|_{V,T,n_2}\left.\frac{\partial\mu_2}{\partial n_2}\right|_{V,T,n_1} - \left.\frac{\partial\mu_1}{\partial n_2}\right|_{V,T,n_1}\left.\frac{\partial\mu_2}{\partial n_1}\right|_{V,T,n_2}\right]\Big/\left.\frac{\partial\mu_2}{\partial n_2}\right|_{V,T,n_1} \quad (2.10)$$

Combining eq 2.10 with eqs 2.6–2.8 yields

$$S_{11}(0)^{-1} = \left[\frac{1}{M_1\phi_1}+\frac{1}{M_2\phi_2}-2g_{12}+\frac{1}{f_S(\phi_\nu)}\left(\frac{1}{M_1M_2\phi_1\phi_2}-2\frac{g_{2\nu}}{M_1\phi_1}-2\frac{g_{1\nu}}{M_2\phi_2}+4g_{1\nu}g_{2\nu}-(g_{12}-g_{1\nu}-g_{2\nu})^2\right)\right]\Big/\left[1+\frac{1}{f_S(\phi_\nu)}\left(\frac{1}{M_2\phi_2}-2g_{2\nu}\right)\right] \quad (2.11)$$

with

$$f_S^{FH} = 1/\phi_\nu \quad (2.12a)$$

$$f_S^{FES}(\phi_\nu) = c\left[\frac{1}{(1-\phi_\nu)[1-(1-\phi_\nu)^{1/3}]}+\frac{1}{3(1-\phi_\nu)^{2/3}[1-(1-\phi_\nu)^{1/3}]^2}\right] \quad (2.12b)$$

$$f_S^{DH}(\phi_\nu) = \left[a'\left(\frac{1}{M_1}+\frac{1}{M_2}\right)+b'\right]\left[\frac{\pi}{2[1-\pi(1-\phi_\nu)/6]^4}-\frac{\pi}{6[1-\pi(1-\phi_\nu)/6]^2}\right] \quad (2.12c)$$

When free volume is absent, we have $\phi_\nu = 0$, and eqs 2.12a–c yields $[f_S(\phi_\nu)]^{-1} = 0$ for the Flory–Huggins and equation of state models. Thus, in these cases eq 2.11 reduces to the well-known RPA formula for an incompressible blend

$$S_{11}(0)^{-1} = \frac{1}{M_1\phi_1}+\frac{1}{M_2\phi_2}-2g_{12} \equiv \frac{1}{M_1\phi_1}+\frac{1}{M_2\phi_2}-2\chi_{eff}^{incomp} \quad (2.13)$$

that provides the customary definition of the effective interaction parameter χ_{eff}^{incomp}. The generalized Flory theory of Dickman and Hall does not produce $[f_S(\phi_\nu=0)]^{-1} = 0$ because excluded-volume repulsion of hard-sphere polymer segments must always leave free volume, even in the limit of closest packing.

Turning now to compressible blends, the effective monomer–monomer interaction parameter, χ_{eff}, is traditionally defined as

$$\chi_{eff} = -\left[S_{11}(0)^{-1}-\frac{1}{M_1\Phi_1}-\frac{1}{M_2\Phi_2}\right]/2 \quad (2.14)$$

where the nominal volume fractions are

$$\Phi_i = \phi_i/(1-\phi_\nu) \qquad i = 1, 2 \quad (2.14a)$$

$$\Phi_1+\Phi_2 = 1 \quad (2.14b)$$

When eq 2.11 is substituted into eq 2.14 and the equation is rearranged, it is found that

$$\chi_{eff} = g_{12} - \frac{\phi_\nu}{2(1-\phi_\nu)}\left[\frac{1}{M_1\Phi_1}+\frac{1}{M_2\Phi_2}\right] + \frac{[M_2\Phi_2(1-\phi_\nu)(g_{12}-(g_{1\nu}-g_{2\nu}))-1]^2}{2M_2\Phi_2(1-\phi_\nu)[1-M_2\Phi_2(1-\phi_\nu)(2g_{2\nu}-f_S(\phi_\nu))]} \quad (2.15)$$

The expression in eq 2.15 can be rewritten in shorthand notation as

$$\chi_{eff} = g_{12} - \frac{\phi_\nu}{2(1-\phi_\nu)}\left[\frac{1}{M_1\Phi_1}+\frac{1}{M_2\Phi_2}\right] + \chi_{eff}^{corr} \quad (2.16)$$

The first two terms in eq 2.16 are exactly the $\chi_{eff}^{incomp,\phi_\nu}$ derived by one of us[5] for an incompressible Flory–Huggins blend with free volume, i.e., with constant ϕ_ν and $g_{1\nu} = g_{2\nu} = 0$. The same results (eq 2.16) also emerge from a generalization of the Edwards style RPA theory to an incompressible blend.[7] The difference between χ_{eff} and $\chi_{eff}^{incomp,\phi_\nu}$ appears in the correction term, χ_{eff}^{corr}, that depends on polymer composition Φ_2, the molecular weight M_2 of the second component, the polymer–polymer interaction g_{12}, $g_{1\nu}$, and $g_{2\nu}$ (see eq 2.2), and the model-dependent free-volume contribution $f_S(\phi_\nu)$ of eq 2.12.

Several limiting forms can readily be derived from the general expression in eq 2.15. The condition $M_2\Phi_2(1-\phi_\nu) \gg 1$ applies for large M_2 and not too small Φ_2. In

this case eq 2.15 simplifies to

$$\chi_{eff} = g_{12} - \frac{\phi_\nu}{2(1-\phi_\nu)}\left[\frac{1}{M_1\Phi_1} + \frac{1}{M_2\Phi_2}\right] + \frac{1}{2[f_S(\phi_\nu) - 2g_{2\nu}]} \times \left[g_{12} - (g_{1\nu} - g_{2\nu}) - \frac{1}{M_2\Phi_2(1-\phi_\nu)}\right]^2 \quad (2.17)$$

If the two polymers have identical polymer–polymer interactions, then $g_{1\nu} = g_{2\nu}$ and eq 2.17 further simplifies to

$$\chi_{eff} = g_{12} - \frac{\phi_\nu}{2(1-\phi_\nu)}\left[\frac{1}{M_1\Phi_1} + \frac{1}{M_2\Phi_2}\right] + \frac{1}{2[f_S(\phi_\nu) - 2g_{2\nu}]} \times \left[g_{12} - \frac{1}{M_2\Phi_2(1-\phi_\nu)}\right]^2 \quad (2.18)$$

On the other hand, when the polymers are quite dissimilar and $|g_{1\nu} - g_{2\nu}| \gg g_{12}$, eq 2.17 reduces to

$$\chi_{eff} = g_{12} - \frac{\phi_\nu}{2(1-\phi_\nu)}\left[\frac{1}{M_1\Phi_1} + \frac{1}{M_2\Phi_2}\right] + \frac{[g_{1\nu} - g_{2\nu}]^2}{2[f_S(\phi_\nu) - 2g_{2\nu}]} \quad (2.19)$$

in which the contribution to χ_{eff} from the correction term in $(g_{1\nu} - g_{2\nu})^2$ may become considerable for large differences $|g_{1\nu} - g_{2\nu}|$.

III. Computation of the Interaction Parameter, χ_{eff}

Equation 2.15 explicitly provides the neutron scattering χ_{eff} for arbitrary concentrations Φ_1 of the compressible binary blend. In order to consider blends in the one-phase region, the parameters g_{12}, $g_{1\nu}$, $g_{2\nu}$, M_1, M_2, and ϕ_ν must be chosen according to the stability conditions[13] described in section IV (see eqs 4.1–4.3). Then a plot of the specific free energy of mixing $\Delta F^{mix}/N_1kT$ against Φ_1 is convex over the whole concentration region, and the pressure is positive for all Φ_1. In a compressible blend the lack of a loop in $\Delta F^{mix}/N_1kT$ versus Φ_1 does not exclude the occurrence of a negative pressure, which may arise when too large a value is chosen for the parameter ϕ_ν. Our computations obtain ϕ_ν approximately from the equation of state for a blend with $\Phi_1 = 0.5$ at 1 atm of pressure to ensure a positive pressure for all Φ_1.

The free energy of mixing is readily obtained from eq 2.1 by subtracting the specific contributions from the pure components 1 and 2

$$\Delta F^{mix}/N_1kT = F/N_1kT - f_1\phi_1 - f_2\phi_2 \quad (3.1)$$

The pressure P is computed as the derivative of F with respect to the number of voids n_ν

$$P \equiv \frac{1}{a^3}\frac{\partial F}{\partial n_\nu}\bigg|_{n_1,n_2,T} = -\frac{1}{a^3}\frac{\partial(\Delta F^{mix})}{\partial n_\nu}\bigg|_{n_1,n_2,T} \quad (3.2)$$

where a^3 denotes the volume of a unit lattice cell. Using F from eq 2.1, P is obtained as

$$P = \frac{kT}{a^3}\left[f_P(\phi_\nu) + \left(\frac{\Phi_1}{M_1} + \frac{\Phi_2}{M_2}\right)(1-\phi_\nu) + g_{12}\Phi_1\Phi_2(1-\phi_\nu)^2 - g_{1\nu}\Phi_1(1-\phi_\nu)^2 - g_{2\nu}\Phi_2(1-\phi_\nu)^2\right] \quad (3.3)$$

where the three different models yield

$$f_P^{FH}(\phi_\nu) = -\ln\phi_\nu - (1-\phi_\nu) \quad (3.4a)$$

$$f_P^{FES}(\phi_\nu) = c(1-\phi_\nu)/[1-(1-\phi_\nu)^{1/3}] \quad (3.4b)$$

$$f_P^{DH}(\phi_\nu) = \left[a\left(\frac{1}{M_1} + \frac{1}{M_2}\right) + b\right]\frac{(1-\phi_\nu)(4\eta - 2\eta^2)}{(1-\eta)^3} \quad (3.4c)$$

where a and b are constant and $\eta \equiv (1-\phi_\nu)\pi/6$. Given choices of polymerization indices M_1 and M_2 (proportional to the molecular weights) and of the energetic parameters g_{12}, $g_{1\nu}$, and $g_{2\nu}$, obtained as described below, values of ϕ_ν are evaluated from eq 3.3 such that $P(\Phi_1) = 1$ atm over the whole concentration range.

Since ϕ_ν appears in eq 2.15 as a parameter, it may be chosen arbitrarily for $\phi_\nu \le \phi_\nu^*(M_1,M_2,g_{ij})$, where ϕ_ν^* prescribes the limits of stability. Alternatively, the equation of state (eq 3.3) may be used to determine $\phi_\nu(\Phi_1)$ for given M_1, M_2, and g_{ij}. Both approaches require a choice of cell volume and temperature. We use $a^3 = (2.5477\ \text{Å})^3$ and specify g_{ij}, rather than ϵ_{ij}, and temperature; but to obtain P we choose $T = 300$ K. However, for all three models over the wide range of M_1, M_2, and g_{ij} considered, the value of ϕ_ν determined from the equation of state for $P = 1$ atm is quite slowly varying with Φ_1 (about 10% variation), and consequently the χ_{eff} values computed with $\phi_\nu(\Phi_1)$ or an average ϕ_ν are nearly identical. Thus, as discussed further below, we use a single average $\bar{\phi}_\nu$. The pressure is very sensitive to even a small change of ϕ_ν and Φ_1. Hence, employing a single average $\bar{\phi}_\nu$ causes the pressure to vary significantly over the whole concentration range (for example, within 250 atm for $M_1 = 100$, $M_2 = 90$, $g_{12} = 0.01$, $g_{1\nu} = 2$, $g_{2\nu} = 2.1$, and $\phi_\nu = 0.06$).

The polymer–polymer model interaction parameter g_{12} in eq 2.2 is a linear combination of three model energies ϵ_{11}, ϵ_{22}, and ϵ_{12}. Computations are performed for g_{12} in the range 10^{-2}–10^{-4} that provides a single phase for the M_1 and M_2 considered. The parameter $g_{1\nu}$ (or $g_{2\nu}$) is related to a single polymer–polymer energy parameter ϵ_{11} (or ϵ_{22}) and is of the order kT because the creation of a void must cost an energy of roughly this magnitude.

Since $\chi_{eff}(\Phi_1)$ is a function of M_1, M_2, g_{12}, $g_{1\nu}$, $g_{2\nu}$, and ϕ_ν, our computations are presented in the form of plots of χ_{eff} versus Φ_1 for a few different values of one chosen parameter, keeping the others unchanged. Figures 1–6 are obtained using Flory–Huggins theory and a Φ_1-independent ϕ_ν.

The influence of ϕ_ν on χ_{eff} is displayed in Figure 1. Smaller ϕ_ν makes g_{12} more closely approach χ_{eff} and makes χ_{eff} less dependent on Φ_1. This behavior is quite understandable: by decreasing the free volume, we approach the limit of an incompressible blend where $\chi_{eff} = g_{12}$ for all Φ_1. Alternatively, this behavior follows from eq 2.15 where the first correction is proportional to ϕ_ν, while $f_S(\phi_\nu)$ in the denominator of the χ_{eff}^{corr} grows as $1/\phi_\nu$ (see eq 2.12) for $\phi_\nu \to 0$.

Figures 2 and 3 show χ_{eff} for various polymerization indices. Larger M_1 and M_2 act in the same direction as smaller ϕ_ν; i.e., they cause χ_{eff} to tend more to g_{12}. This behavior follows from the M_i^{-1} dependence of the corrections in eqs 2.15 and 2.17 so long as $g_{1\nu}$ does not greatly depart from $g_{2\nu}$. Large differences between M_1 and M_2 make χ_{eff} more asymmetrical as a function of Φ_1. Various values of g_{12} produce corresponding χ_{eff} (see Figure 4) that are close to the respective g_{12} for $\Phi_1 = 0.5$ and g_{12} in the higher ranges. If g_{12} is sufficiently small, the corrections make g_{12} depart more considerably from χ_{eff}, which now can be negative over the whole concentration range. This behavior arises from eq 2.16 when the second term dominates and determines the sign of χ_{eff}.

The curves $\chi_{eff}(\Phi_1)$ in Figures 1–4 are all computed for the energetical parameters $g_{1\nu} = 2$ and $g_{2\nu} = 2.1$. When we take $g_{1\nu}$ and $g_{2\nu}$ to be equal, the curves remain practically unchanged, and $\chi_{eff}(\Phi_1=0.5)$ is still close g_{12} unless g_{12} is very small. Values of $g_{1\nu}$ and $g_{2\nu}$ that differ, for example, by as much as as unity generate χ_{eff} much greater

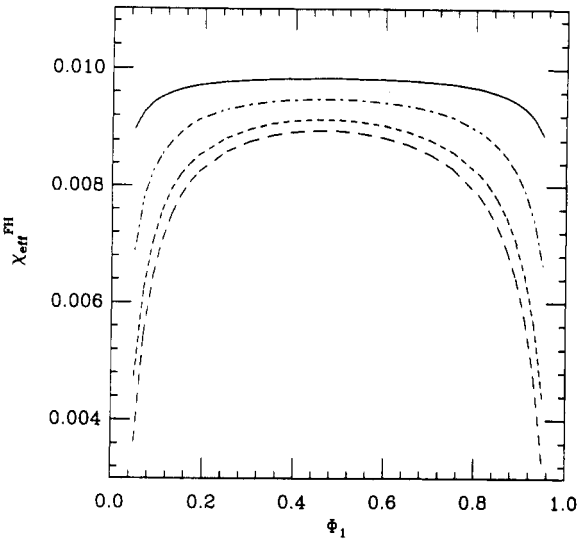

Figure 1. Flory–Huggins effective interaction parameter, χ_{eff}^{FH}, for compressible binary blend as a function of the nominal volume fraction, Φ_1, of component 1 for $M_1 = 100$, $M_2 = 90$, $g_{12} = 0.01$, $g_{1\nu} = 2$, $g_{2\nu} = 2.1$, and various values of the volume fraction ϕ_ν of voids. The solid curve corresponds to $\phi_\nu = 0.01$, the dot-dashed curve to $\phi_\nu = 0.03$, the short dash curve to $\phi_\nu = 0.05$, and the long dash curve to $\phi_\nu = 0.06$.

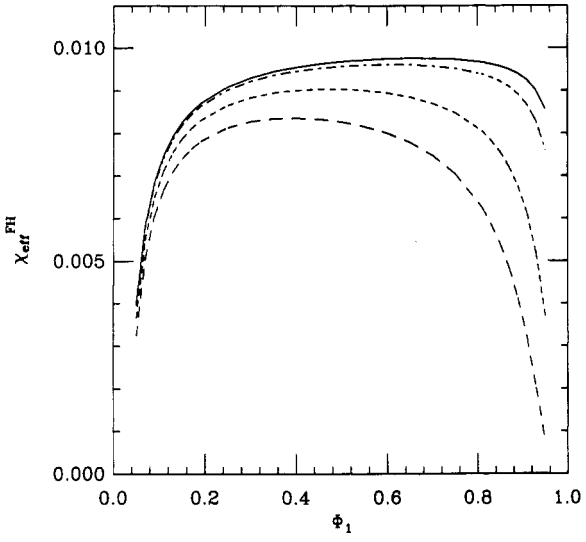

Figure 2. Same as Figure 1 for $M_1 = 100$, $g_{12} = 0.01$, $g_{1\nu} = 2$, $g_{2\nu} = 2.1$, $\phi_\nu = 0.06$, and various values of the polymerization index, M_2, of component 2. The solid curve is for $M_2 = 500$, the dot-dashed curve for $M_2 = 300$, the short dash curve for $M_2 = 100$, and the long dash curve for $M_2 = 50$.

than g_{12} (see Figures 5 and 6). Note that the shape of the curves changes when the difference $g_{1\nu} - g_{2\nu}$ is positive and sufficiently large (see Figure 5).

Equation 2.15 exhibits a dependence on the three models only through the factor of $f_S(\phi_\nu)$ in the denominator of the last term. The limits in eqs 2.17–2.19 indicate that this contribution is largest for large differences $|g_{1\nu} - g_{2\nu}|$, but in actual calculations the three models yield very similar $\chi_{eff}(\Phi_1)$ when $g_{1\nu}$ and $g_{2\nu}$ are properly scaled between the models to yield the same pressures for given M_1, M_2, g_{12}, and ϕ_ν. For instance, in the Dickman–Hall model it is necessary to use much higher $g_{1\nu}$ and $g_{2\nu}$ (between 7.45 and 6.45 instead of the range 2–1 for the Flory–Huggins model). The equation of state model has the extra adjustable parameter c that may be chosen for arbitrary values of $g_{1\nu}$ and $g_{2\nu}$ to reproduce very closely the Flory–Huggins $\chi_{eff}(\Phi_1)$ curves. Hence, the χ_{eff} values evaluated for the Flory–Huggins model are universal in the

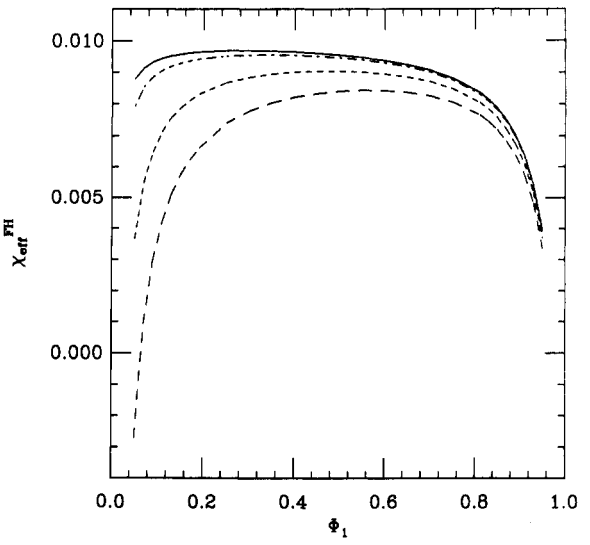

Figure 3. Same as Figure 1 for $M_2 = 100$, $g_{12} = 0.01$, $g_{1\nu} = 2$, $g_{2\nu} = 2.1$, $\phi_\nu = 0.06$, and various values of the polymerization index, M_1, of component 1. The solid curve is for $M_1 = 500$, the dot-dashed curve for $M_1 = 300$, the short dash curve for $M_1 = 100$, and the long dash curve for $M_1 = 50$.

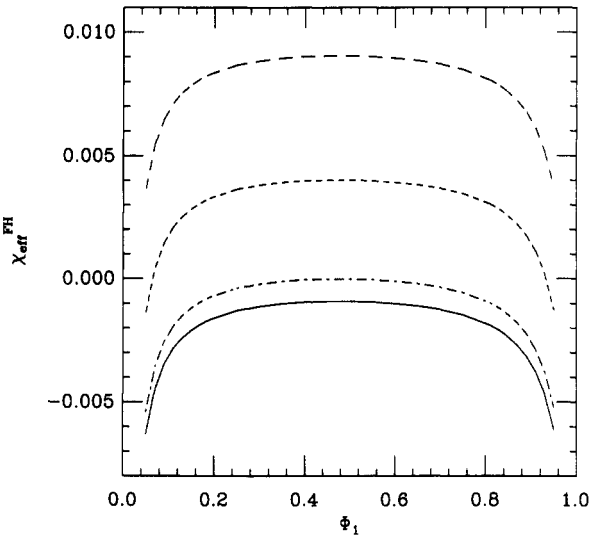

Figure 4. Same as Figure 1 for $M_1 = M_2 = 100$, $g_{1\nu} = 2$, $g_{2\nu} = 2.1$, $\phi_\nu = 0.06$, and various values of the interaction parameter g_{12}. The solid curve corresponds to $g_{12} = 0.0001$, the dot-dashed curve to $g_{12} = 0.001$, the short dash curve to $g_{12} = 0.005$, and the long dash curve to $g_{12} = 0.01$.

sense that their general shapes do not depend on which of the three models of free volume is employed.

Considerable effort is currently being devoted to small-angle neutron-scattering experiments on polymer blends in order to extract the effective interaction parameter, χ_{eff}, that is believed to provide molecular information on basic polymer–polymer interactions and thereby yield insight into molecular characteristics promoting mixing of blends or particular morphologies in phase-separated systems. However, this approach is only as adequate as the theoretical models used to analyze the experimental data. If, as we demonstrate here, the theoretical models (e.g., incompressible RPA) do not appropriately reflect the actual physical situation, then the extracted χ_{eff} from these models contains spurious dependences on molecular weights and blend composition.

Small-angle neutron-scattering experiments are generally analyzed using an incompressible RPA model whose extrapolated zero-angle limit is already obviously in conflict with the wide body of literature on models of equa-

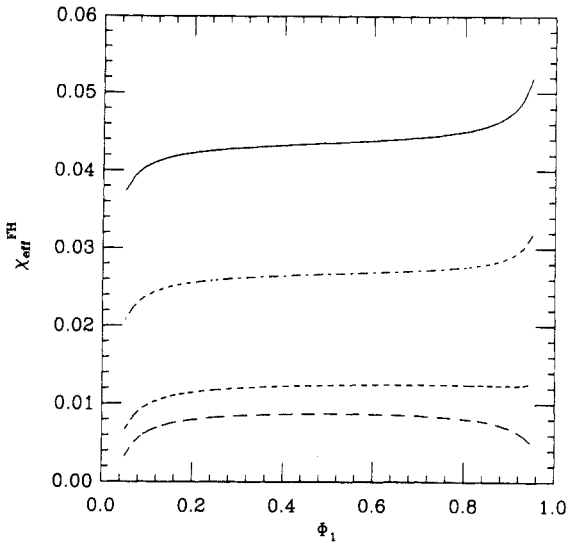

Figure 5. Same as Figure 1 for $M_1 = M_2 = 100$, $g_{12} = 0.01$, $g_{1\nu} = 2$, $\phi_\nu = 0.06$, and various values of the interaction parameter $g_{2\nu}$. The solid curve is for $g_{2\nu} = 1$, the dot-dashed curve for $g_{2\nu} = 1.3$, the short dash curve for $g_{2\nu} = 1.7$, and the long dash curve for $g_{2\nu} = 2$.

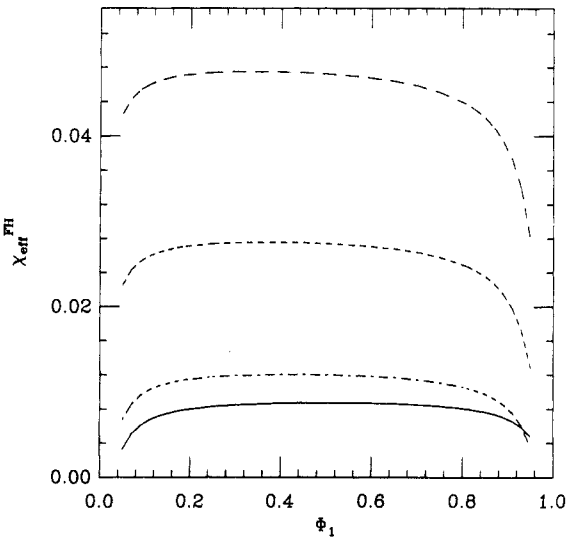

Figure 6. Same as Figure 1 for $M_1 = M_2 = 100$, $g_{12} = 0.01$, $g_{2\nu} = 2$, $\phi_\nu = 0.06$, and various values of the interaction parameter $g_{1\nu}$. The solid curve refers to $g_{1\nu} = 2$, the dot-dashed curve to $g_{1\nu} = 1.7$, the short dash curve to $g_{1\nu} = 1.3$, and the long dash curve to $g_{1\nu} = 1$.

tion of state for blends. We use the *simplest* of the available thermodynamics models of polymer blends to demonstrate the spurious behavior exhibited by the incompressible RPA analysis for χ_{eff}. Our main point is that meaningful polymer–polymer interaction parameters must be extracted from experimental data by using faithful models of the blend thermodynamics.

IV. Computation of Spinodal Diagrams

The spinodal line for the limits of stability for a homogeneous one-phase blend is often estimated by using the experimentally determined χ_{eff} in eq 2.14 with the condition $[S_{11}(0)]^{-1} = 0$. In view of the questions raised in section III concerning the appropriateness for real blends of the conventional definition (eq 2.14) for χ_{eff}, we now analyze the accuracy of such an approach for compressible blends by contrasting this stability analysis with that dictated by thermodynamic considerations.

For a compressible binary blend at constant volume V, the existence of a stable (or metastable) homogeneous phase requires the following conditions[13]

$$f_{\phi_i\phi_i} > 0 \qquad i = 1, 2 \tag{4.1}$$

$$f_{\phi_1\phi_1} f_{\phi_2\phi_2} - f_{\phi_1\phi_2} f_{\phi_2\phi_1} > 0 \tag{4.2}$$

where

$$f_{\phi_i\phi_j} \equiv \left.\frac{\partial^2(F/N_1)}{\partial\phi_i\,\partial\phi_j}\right|_{V,T} \qquad i, j = 1, 2 \tag{4.3}$$

is the second derivative of the specific Helmholtz free energy F/N_1 (see eq 2.1) with respect to the volume fractions ϕ_i and ϕ_j. When taking the derivative in eq 4.3, the volume fraction ϕ_ν of voids is not held constant as we have $d\phi_i = -d\phi_\nu$ at fixed ϕ_j ($j \neq i$) and volume. Using eqs 2.1 and 2.3, the conditions in eqs 4.1 and 4.2 take the form

$$\frac{1}{\phi_\nu} + \frac{1}{M_i\phi_i} - 2g_{i\nu} > 0 \qquad i = 1, 2 \tag{4.4}$$

$$\left[\frac{1}{\phi_\nu} + \frac{1}{M_1\phi_1} - 2g_{1\nu}\right]\left[\frac{1}{\phi_\nu} + \frac{1}{M_2\phi_2} - 2g_{2\nu}\right] - \left[\frac{1}{\phi_\nu} + g_{12} - g_{1\nu} - g_{2\nu}\right]^2 > 0 \tag{4.5}$$

When the left-hand side of the inequality eq 4.5 is set equal to zero, the equation governing the spinodal line is determined as

$$\left[\frac{1}{\phi_\nu} + \frac{1}{M_1\phi_1} - 2g_{1\nu}\right]\left[\frac{1}{\phi_\nu} + \frac{1}{M_2\phi_2} - 2g_{2\nu}\right] - \left[\frac{1}{\phi_\nu} + g_{12} - g_{1\nu} - g_{2\nu}\right]^2 = 0 \tag{4.6}$$

It is easy to show that eq 4.6 is equivalent to the vanishing of the reciprocal of the partial structure factor[6] $[S_{11}(0)]^{-1}$ (see eq 2.11)

$$[S_{11}(0)]^{-1} = 0 \tag{4.7}$$

Thus, a combination of the traditional RPA analysis of χ_{eff}, with an extrapolation to find the conditions for which eq 4.7 applies, provides a consistent approach for determining the constant-*volume* spinodal of a compressible blend, despite the apparent inconsistency of appearing to ignore blend compressibility throughout the analysis. On the other hand, many experiments on the thermodynamics of phase separation are performed at constant *pressure*, not constant volume, and we now consider how accurately the conditions eq 4.6 and 4.7 approximate the constant-pressure spinodal.

A compressible binary blend at constant pressure has volume fluctuations. It is more convenient in this case to determine the phase stability criteria in terms of derivatives of the Gibbs free energy, G. This condition is

$$\left.\frac{\partial^2 G}{\partial\Phi_1^2}\right|_{T,P} > 0 \tag{4.8}$$

where Φ_1 is defined by eq 2.14 as the nominal volume fraction of component 1. Combining eqs 2.6 and 2.7 together with the equation of state (eqs 3.3 and 3.4) and the thermodynamic identity

$$\left.\frac{\partial\mu_i}{\partial n_j}\right|_{T,P,n_i} = \left.\frac{\partial\mu_i}{\partial n_j}\right|_{T,V,n_i} - \frac{v_i v_i}{V\kappa} \tag{4.9}$$

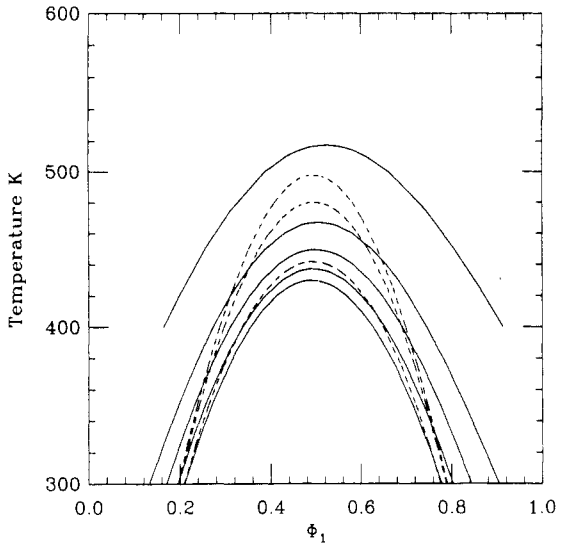

Figure 7. Comparison of spinodal lines for a compressible binary blend at constant volume with ϕ_ν = 0.3, 0.2, 0.15, 0.1, and 0.05 (solid lines: top to bottom, respectively) and at the constant pressures P = 1000, 100, and 1 atm (dashed lines: top to bottom, respectively). All curves are calculated for polymerization indices M_1 = 100 and M_2 = 90 and the interaction parameters $g_{12} = 0.03(300/T)$, $g_{1\nu} = 2.0(300/T)$, and $g_{2\nu} = 1.7(300/T)$. The critical points are slightly displaced from $\Phi_1 = 0.5$.

where κ is the isothermal compressibility

$$\kappa \equiv -\frac{1}{V}\frac{\partial V}{\partial P}\bigg|_{T,n_1,n_2} \tag{4.9a}$$

and ν_i is the partial volume of component i

$$\nu_i = \frac{\partial V}{\partial n_i}\bigg|_{T,P,n_j} \tag{4.9b}$$

the stability condition (eq 4.8) translates into the equation for the spinodal line at constant P

$$\left[\frac{2}{\phi_\nu} + \frac{1}{M_1(1-\phi_\nu)} + \frac{1}{M_2(1-\phi_\nu)} + g_{12} - g_{1\nu}(1+2\Phi_1) - g_{2\nu}(1+2\Phi_2)\right] \times \left[\frac{1}{M_1(1-\phi_\nu)} - \frac{1}{M_2(1-\phi_\nu)} + g_{12}(1-2\Phi_1) - g_{1\nu} + g_{2\nu}\right] - \left[\frac{1}{\phi_\nu} + \left(\frac{\Phi_1}{M_1} + \frac{\Phi_2}{M_2}\right)\frac{1}{1-\phi_\nu} + 2(g_{12}\Phi_1\Phi_2 - g_{1\nu}\Phi_1 - g_{2\nu}\Phi_2)\right] \times \left[\frac{1}{M_1(1-\phi_\nu)\Phi_1} - \frac{1}{M_2(1-\phi_\nu)\Phi_2} - 2g_{1\nu} + 2g_{2\nu}\right] = 0 \tag{4.10}$$

The eqs 4.4 and 4.10 for spinodals at constant V and constant P, respectively, are different, and therefore, in principle, upon use of eq 2.2 they permit the construction of approximate but differing phase diagrams $T = T(\Phi_1)$. Figure 7 contrasts the spinodal diagrams at constant V (solid lines) and the spinodal diagrams at constant P (dashed lines) for the following set of parameters: $g_{12} = 0.03(300/T)$, $g_{1\nu} = 2(300/T)$, $g_{2\nu} = 1.7(300/T)$, $M_1 = 100$, and $M_2 = 90$. In constructing the constant-pressure spinodals, the volume fractions ϕ_ν of voids are determined from equation of state (eq 3.3) with a = 2.5477 Å. Thus, it is necessary to solve both eqs 4.10 and 3.3 for given P simultaneously to obtain the coexisting phases with Φ_1', $\Phi_2' = 1 - \Phi_1'$, and ϕ_ν' and with Φ_1'', $\Phi_2'' = 1 - \Phi_1''$, and ϕ_ν''. This is accomplished iteratively by use of the input guess of ϕ_ν generating from $P(\Phi_1{=}0.5)$. For temperatures below critical point this procedure rapidly converges after a few steps, ensuring thermodynamic consistency.

To generate the spinodals at constant V, we simply take ϕ_ν as a constant.

The spinodal diagrams (Figure 7) at constant V and at constant P have similar parabolic shapes, but they are quite different. They are not symmetric about $\Phi_1 = 0.5$, and the critical point does not have $\Phi_1 = 0.5$. The critical temperatures at constant P vary with P just as the critical temperatures at constant V vary with ϕ_ν. Consequently, the spinodal line predicted on the basis of an RPA analysis of small neutron scattering may be quite inaccurate for predicting the spinodal in constant-pressure experiments.

V. Discussion

We analyze simple thermodynamic models of a binary compressible blend. Compressibility dictates that there are three independent interaction parameters. The latter may be polymer–polymer and polymer–void model parameters g_{12}, $g_{1\nu}$, and $g_{2\nu}$ that are assumed, for simplicity, to be independent of composition and of individual monomer molecular structure. In reality, all three parameters are functions of the volume fractions ϕ_1 and ϕ_2 and the monomer molecular structures of both components.[14]

The assumption of composition-independent g_{ij} is used here to focus attention on the inadequacy of the incompressible RPA analysis of χ_{eff}. A more thorough solution of the lattice model of polymer blends than that of Flory–Huggins theory shows that each g_{ij}, in general, contains an entropic portion as well as an energy part with separate rich molecular structure and composition dependences.[14] Such a general and more realistic description of the compressible blend is much more complex than the simplest analysis given here, but it will be studied in the future to provide insight on the molecular structure dependence of χ_{eff}.

We use the traditional RPA analysis to extract χ_{eff} from the zero-angle coherent scattering that is computed from Flory–Huggins, equation of state, and Dickman–Hall type models. The computed χ_{eff} values exhibit strong composition and molecular weight dependences *solely* as a result of the inappropriate incompressible RPA analysis. In some instances, χ_{eff} even has the opposite sign from the input polymer–polymer interaction parameter g_{12}. Considering that the χ_{eff} values, obtained from an incompressible RPA analysis, are often used in theories of phase-separation dynamics, interfacial profiles, etc., internal consistency of the χ_{eff} values between different phenomena does not necessarily justify the original incompressibility model. Rather, the models may be consistent but wholly inadequate to represent the actual physical situation. An example of the latter is provided by our analysis of the RPA-based estimation of spinodals.

Our computed χ_{eff} values are invariant to the choices taken for the entropy associated with free volume (over the range parameters studied), and the χ_{eff} curves display sharp composition dependences that mirror some experimental χ_{eff}. However, our computations yield concave down and down-flat-up shapes for χ_{eff}. This does not, however, produce the convex-up dependences observed experimentally. On the other hand, the theory of corrections to the simple Flory–Huggins approximation[10,14] displays a strong composition and monomer structure dependent to the input g_{12}, $g_{1\nu}$, and $g_{2\nu}$, and this likely induces considerable extra structure to χ_{eff} that will be described elsewhere.

The main conclusion of our simple analysis is that a one-interaction-parameter description of polymer blends produces a gross oversimplification of the actual physical systems. Hence, these incompressible blend models obscure some molecular factors governing blend miscibility, phase separation, etc. Desired molecular information on effective interaction parameters can be extracted from experimental data by using more realistic models of blend thermodynamics. Unfortunately, these more realistic models are, of necessity, many parameter models requiring considerably more input data for determination of the desired molecular interaction parameters. The three models studied here are approximate, but they are far superior to the incompressible blend model that is most widely used to extract and interpret χ_{eff}. Use of even better models to analyze experiments should produce physically more meaningful molecular interaction parameters.

The experimental parameter χ_{eff} is usually calculated from the observed scattering $S_{exp}(\mathbf{q})$ by subtracting[16] a weighted average of the scatterings $S^{(i)}(\mathbf{q})$ corresponding to pure components

$$S(\mathbf{q}) = S_{exp}(\mathbf{q}) - \phi_1 S^{(1)}(\mathbf{q}) - \phi_2 S^{(2)}(\mathbf{q}) \qquad (5.1)$$

in order to remove approximately contributions from density fluctuations. The volume fraction, ϕ_i, in eq 5.1 may be represented by either the nominal volume fraction, Φ_i, or experimental volume fraction, $\Phi_i^{exp} = V_i/(V_1 + V_2)$. Subtracting the contributions of pure components of blend from $S_{11}(0)$ and/or using ϕ_i^{exp} do not qualitatively change the concave-down shape of curves $\chi_{eff}(\Phi_1)$ or $\chi_{eff}(\phi_1^{exp})$; strong molecular weight and composition dependences are maintained. We may also account for the differing scattering lengths and express the total scattering by a compressible blend as

$$S(0) = p_1^2 S_{11}(0) + 2p_1p_2S_{12}(0) + p_2^2 S_{22}(0) \qquad (5.2)$$

where p_1 and p_2 are reduced scattering lengths normalized such that $p_1 - p_2 = 1$. Again, use of eq 5.2 with or without the subtraction of eq 5.1, etc., does not alter the general qualitative conclusions described in the previous paragraph, namely χ_{eff} is molecular weight and composition dependent within our model of calculations solely because of the use of the incompressible RPA to analyze a compressible system.

Given the inadequacy of the RPA theory in representing the zero-angle scattering data, it becomes natural to question whether the $\mathbf{q}$ dependence of this RPA model is likewise grossly deficient. A recent compressible RPA calculation by McMullen and Freed[7] recovers the first correction term in eq 2.16 but misses χ_{eff}^{corr} because of explicit neglect of the free energy cost of introducing free volume into the system. This suggests modification[15] of the Edwards style models and RPA calculations to bring them in line with known thermodynamics of blends.

Experimental estimates of the spinodal are obtained using empirically determined χ_{eff} from the RPA analysis and the *incompressible* blend spinodal condition $[S_{11}(0)]^{-1} = 0$. Despite the apparent inconsistency of this procedure for actual compressible blends, we demonstrate that this process correctly provides the constant-volume spinodal. However, many experiments on phase behavior of blends are performed at constant pressure, and the constant-pressure spinodals can be quite different from their constant-volume counterparts. In the example considered the shapes of the curves are similar, but the critical temperatures differ. Both cases yield only a single spinodal curve. We expect that a second one will emerge upon introduction of the composition and molecular structure dependence of the g_{ij}, and considerable interest in lower solution critical points provides one strong motivation for studying these richer models of the g_{ij}.

Theories of coherent scattering from polymer blends are significantly more difficult than are statistical thermodynamic theories of blends. Since the extrapolated zero-angle coherent scattering is a thermodynamic quantity, the better known blend thermodynamics should be applied in this limit if the objective is to obtain fundamental information concerning the molecular interactions in a blend that govern miscibility and phase diagrams. Our contrasting of the predictions of a standard incompressible RPA analysis with the actual physical situation, as represented by a simple input model, indicate that blend compressibility strongly affects the interpretation of the data and further suggests the need for improvement[15] in theories of the coherent scattering such that the limiting zero-angle scattering be consistent with a more realistic description of the blend thermodynamics.

Acknowledgment. This research is supported, in part, by NSF Grant No. DMR86-14358 and a grant from the donors of Petroleum Research Fund, administered by the American Chemical Society. We are grateful to Bill McMullen, Stuart Rice, and Davis Walsh for helpful discussions.

References and Notes

(1) de Gennes, P.-G. *Scaling Concepts in Polymer Physics*; Cornell University Press: Ithaca, NY, 1979.
(2) Flory, P. J. *J. Chem. Phys.* **1941**, *9*, 660; **1942**, *10*, 51. *Principles of Polymer Chemistry*; Cornell University Press: Ithaca, NY, 1953. Huggins, M. L. *J. Chem. Phys.* **1941**, *9*, 440; *J. Phys. Chem.* **1942**, *46*, 151; *Ann. N.Y. Acad. Sci.* **1943**, *44*, 431.
(3) *Polymer Handbook*; Brandup, J., Immergut, E. H., Eds., Wiley: New York, 1975.
(4) Flory P. J. *Discuss. Faraday Soc.* **1970**, *49*, 7. Sanchez, I. C.; Lacombe, R. H. *Macromolecules* **1978**, *11*, 1145. Panayiotou, C. G. *Ibid.* **1987**, *20*, 861. Koningsveld, R.; Kleintjens, L. A.; Leblans-Vinck, A. M. *J. Phys. Chem.* **1987**, *91*, 6423. Dee, G. T.; Walsh, D. J. *Macromolecules* **1988**, *21*, 811, 815. Walsh, D. J.; Dee, G. T.; Halary, J. L.; Ubiche, J. M.; Millequant, M.; Lesec, J.; Monnerie, L. *Macromolecules* **1989**, *22*, 3395.
(5) Freed, K. F. *J. Chem. Phys.* **1988**, *88*, 5871.
(6) Sariban, A.; Binder, K. *J. Chem. Phys.* **1987**, *86*, 5859.
(7) McMullen, W. E.; Freed, K. F. *Macromolecules*, in press.
(8) Dickman, R.; Hall, C. K. *J. Chem. Phys.* **1986**, *85*, 4108.
(9) Bates, F. S.; Muthukumar, G. D.; Wignall, G. D.; Fetters, L. J. *J. Chem. Phys.* **1988**, *89*, 535. Bates, F. S.; Fetters, L. J.; Wignall, G. D. *Macromolecules* **1988**, *21*, 1086. Maconnachie, A.; Kambour, R. P.; White, D. M.; Rostami, S.; Walsh, D. J. *Ibid.* **1984**, *17*, 2645. Ito, H.; Russel, T. P.; Wignall, G. D. *Macromolecules* **1987**, *20*, 2213. Murray, C. T.; Gilmer, J. W.; Stein, R. S. *Ibid.* **1985**, *18*, 996. Han, C. C.; Bauer, B. J.; Clark, J. C.; Muroga, Y.; Matsushita, Y.; Okada, M.; Tran-Cong, Q.; Sanchez, I. C. *Polymer* **1988**, *29*, 2003.
(10) Freed, K. F.; Bawendi, M. G. *J. Phys. Chem.* **1989**, *93*, 2194. Bawendi, M. G.; Freed, K. F.; Mohanty, U. *J. Chem. Phys.* **1987**, *87*, 5534. Bawendi, M. G.; Freed, K. F. *Ibid.* **1988**, *88*, 2741. Nemirovsky, A. M.; Bawendi, M. G.; Freed, K. F. *Ibid.* **1987**, *87*, 7272. Pesci, A. I.; Freed, K. F. *Ibid.* **1989**, *90*, 2003.
(11) Carnahan, N. F.; Starling, K. E. *J. Chem. Phys.* **1969**, *51*, 635.
(12) Honnell, K. G.; Hall, C. K. *J. Chem. Phys.* **1989**, *90*, 1841.
(13) Sanchez, I. C. Statistical Thermodynamics of Polymer Solutions. In *Introduction to Theoretical Polymer Physics*, Lecture notes for the Division of High Polymer Physics Short Course, March 14–15, 1987; *Am. Phys. Soc.*, unpublished. Sanchez, I. C.; Balazs, A. C. *Macromolecules* **1989**, *22*, 2325.
(14) See, for example: Pesci, A. I.; Freed, K. F. *J. Chem. Phys.* **1989**, *90*, 2017. Madden, W. G.; Pesci, A. I.; Freed, K. F. *Macromolecules*, in press. Dudowicz, J.; Freed, K. F.; Madden, W. G., submitted for publication in *Macromolecules*.
(15) Tang, H.; Freed, K. F., to be published.
(16) Shibayama, M.; Yang, H.; Stein, R. S.; Han, C. C. *Macromolecules* **1985**, *18*, 2179.

Registry No. Neutron, 12586-31-1.